Letters

Online Frequency Response Measurements of Grid-Connected Systems in Presence of Grid Harmonics and Unbalance

Roni Luhtala, Henrik Alenius, Tuomas Messo, and Tomi Roinila

***Abstract*—Grid characteristics have a drastic impact on the stability and control performance of grid-connected systems. Because the grid conditions typically vary over time, online measurements are most desirable for the stability assessment, protection design, and control system optimization of the systems. Previous studies have presented methods based on Fourier techniques and broadband sequences, with which the frequency responses of the grid-connected systems, such as the grid impedance or inverter control loops, can be measured. However, online measurements under unbalanced grids with harmonic voltages have not been comprehensively considered. This letter demonstrates how the previously applied online measurement methods fail in the presence of unbalanced grid and voltage harmonics due to the spectral leakage caused by the Fourier transform. This letter also proposes a simple signal design method to avoid the leakage. Experimental results based on a high-power grid-connected system are shown to demonstrate the effectiveness of the proposed method.**

***Index Terms*—Discrete fourier transforms, frequency response, measurement errors, power system identification, spectral analysis.**

I. Introduction

THE performance and stability of grid-connected power electronics applications are significantly affected by the interfaced grid [1]–[4]. Since the grid conditions vary over time, online measurements of the grid impedance and the load-affected converter ac-side dynamics are most desirable for obtaining the system stability margins in the grid connection point. Additionally, online measurements acquired in real time allow novel control strategies, such as adaptive control or adjustment of the protection parameters. Such measurements have become popular in power electronics applications, including grid-connected converters [5]–[8]. In most of the presented methods, a broadband perturbation, such as pseudorandom binary sequence (PRBS) is injected into the system, and the Fourier analysis is applied to extract the corresponding frequency components in the responses.

A single converter may face unpredictable grid conditions, such as a weak grid or poor grid voltages [2], [9]. The disturbances in grid voltages, such as voltage harmonics, may cause errors in the frequency response measurements. Although the issues related to unbalanced or harmonic-polluted grid voltages are widely known, the impact of the voltage waveforms on the online measurements has not been previously considered. This letter discusses the measurement issues under the unbalanced grid with a high harmonic content and introduces a design procedure of the perturbation signal to suppress the issues.

The grid harmonics appear as periodic oscillations in the measured samples. When the discrete Fourier transform (DFT) is applied, the periodic oscillations may leak to other frequencies through two undesired features known as the spectral leakage and the picket fence effect (PFE) [5], [10]. The PFE appears if the discrete spectrum, produced by the DFT, does not include exactly the frequencies of periodic oscillations. This results in leaking to the nearest available frequency bins [11]. The spectral leakage occurs when the DFT is applied on samples that contain noninteger periods of periodic signals, causing those frequencies to leak over a wide frequency band [12].

The grid fundamental and its harmonics appear at specific frequencies. This means they can be taken into account when adjusting the measurement time so that each measured sample contains integer periods of the grid fundamentals, and thereby, also its harmonics. This suppresses the spectral leakage caused by grid harmonics and unbalance.

This letter shows how the spectral leakage deteriorates the online frequency response measurements under grid harmonics and unbalance. It also introduces a design procedure to remove the spectral leakage from the measurements.

The remainder of this letter is organized as follows. Section II reviews the online frequency response measurements and issues related to the spectral leakage. Section III introduces the applied broadband perturbations that are suitable for the *dq*-domain measurements and proposes a design procedure for measurements under the grid unbalance and harmonics. Section IV shows high-power experimental results, in which spectral leakage occurs,

Manuscript received August 19, 2019; revised September 11, 2019; accepted September 22, 2019. Date of publication September 24, 2019; date of current version January 10, 2020. This work was supported in part by the European Union's Horizon 2020 Research and Innovation Programme under Grant 654113, in part by the European Research Infrastructure ERIGrid and its partner DNVGL, and in part by the Academy of Finland. *(Corresponding author: Roni Luhtala.)*

R. Luhtala and T. Roinila are with the Department of Automation and Hydraulics, Tampere University, 33014 Tampere, Finland (e-mail: roni.luhtala@tuni.fi; tomi.roinila@tuni.fi).

H. Alenius and T. Messo are with the Laboratory of Electrical Energy Engineering, Tampere University, 33720 Tampere, Finland (e-mail: henrik.alenius@tuni.fi; tuomas.messo@tuni.fi).

Color versions of one or more of the figures in this article are available online at http://ieeexplore.ieee.org.

Digital Object Identifier 10.1109/TPEL.2019.2943711

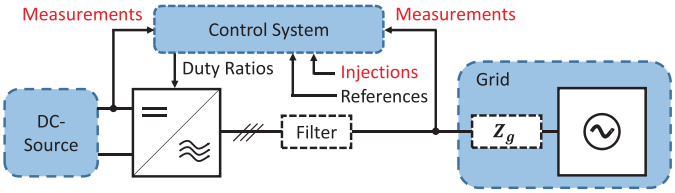

Fig. 1. Grid-connected inverter.

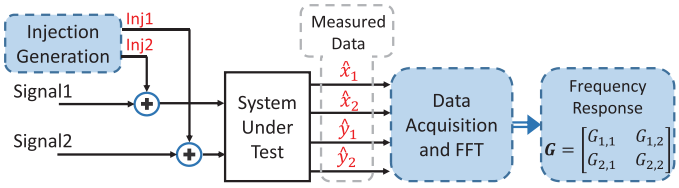

Fig. 2. Typical frequency response measurement setup.

and how the proposed design procedure can be used to remove the leakage. Section V draws the conclusion.

II. Online Measurements of Grid-Connected Systems

Fig. 1 shows a three-phase grid-connected inverter. The inverter is controlled based on measurements from the dc- and ac-side waveforms. The same measurements can be used for the frequency response identification, which usually requires an excitation signal to be injected into the system. A typical frequency response measurement setup for the multi-input multi-output (MIMO) identification is illustrated in Fig. 2. In this example, two signals are perturbed, the system responses are measured, and the frequency response is computed using Fourier techniques [7]. The online measurements can be performed either for the grid- or the inverter-side transfer functions, thus obtaining, for example, the grid impedance or inverter control loops.

Three-phase grid-connected systems are often analyzed in the dq domain, where three-phase ac quantities can be transformed into two dc quantities, d and q components [1]. In the dq domain, full-order transfer functions are represented as 2×2 matrices that include direct (dd and qq) and cross-coupling (dq and qd) components. The dq-domain measurements can be performed in accordance with the setup shown in Fig. 2, where Signal1 and Signal2 correspond to the d and q components. In the computed frequency response matrix, the diagonal components ($G_{1,1}$ and $G_{2,2}$) usually refer to direct components (G_{dd} and G_{qq}) and the off-diagonal components ($G_{1,2}$ and $G_{2,1}$) refer to crosscouplings (G_{dq} and G_{qd}).

In online measurements of the grid-connected systems, the grid cannot be considered as an ideal three-phase voltage source, due to the occurrence of nonidealities, such as harmonics, unbalance, or noise. The measurement noise is usually relatively low and can be mitigated by simply increasing the signal-to-noise ratio (SNR) of the measurements by applying the higher perturbation amplitude or by averaging the measurements over multiple measurement cycles [10].

The grid harmonics and unbalance appear as periodic oscillations in the measured data. When the DFT is applied, two unwanted features may appear: spectral leakage and PFE [12]. These features deteriorate the spectral estimation and may cause drastic errors in the frequency response measurements [5], especially at frequencies near the grid voltage harmonics. The PFE results from noncoherent sampling as a discrete spectrum of the DFT does not include exactly the same frequencies that appear in the measured data, causing these frequencies to leak to the nearest frequency bins. The spectral leakage appears if the measured time-domain data do not include exact integer periods of each periodic signal components, such as the grid voltage fundamental and its harmonics. If the DFT sample contains fractional periods of periodic signals, the DFT interprets them as discontinuations that cause spectral leakage over a wide frequency band.

III. Measurement Design

A. Orthogonal Pseudorandom Sequences

A maximum-length binary sequence (MLBS) is a widely applied broadband excitation in the frequency response measurements of power electronics systems [5]. The MLBS can be easily modified; the sequence has the lowest possible crest factor and is periodic over its length $N = n^2 - 1$, where n is an integer [10]. Considering the measurement setup shown in Fig. 2, one can apply orthogonal binary sequences for simultaneously measuring the full impedance matrix [6], [7]. In the method, two orthogonal sequences are simultaneously injected into d and q channels. As the injections have energy at different frequencies, several (coupled) impedance components can be measured during a single measurement cycle.

The work in [6] and [7] applied a method based on Hadamard modulation for generating orthogonal binary sequences. In the method, the conventional MLBS is used as a first injection. The second (orthogonal) injection is obtained by doubling the MLBS and inverting every other digit. Due to inverse-repeated characteristics of the second injection, the power of the even-order harmonics equals to zero and, thus, must be neglected from the frequency response measurements [6].

B. Measurement Parameters

The optimal online measurement design avoids unnecessarily long measurement time and high injection amplitude, while still providing the sufficient SNR. Averaging reduces the effect of the noise, but the spectral leakage may still remain. The leakage can be minimized by designing the measurement setup so that an integer number of the grid fundamental cycles (and, thereby, also its harmonics) occurs in the measured sample. The number of the grid fundamental cycles that occur during the measurement time can be given as

$$\frac{N}{f_{\text{gen}}} P f_{\text{g}} = (R + r) \tag{1}$$

where P is a number of averaged MLBS (generated at f_{gen}) periods and f_{g} is a grid fundamental frequency. The number of

grid fundamental cycles is separated to its integer part (R) and fractional part (r), from which the nonzero r causes the spectral leakage. The time difference ΔT between the measurement time and the nearest multiple of the periodic cycle can be given as

$$\Delta T = \text{abs}\left[\frac{N}{f_{\text{gen}}}Pf_{\text{g}} - \text{round}\left(\frac{N}{f_{\text{gen}}}Pf_{\text{g}}\right)\right]\frac{1}{f_{\text{g}}} \tag{2}$$

where the operator $round$ gives the nearest integer of the grid fundamental. By varying the averaged periods, the local minimum of the spectral leakage is expected when $\Delta T(P)$ (and r) is minimized, representing the proposed measurement design. The following design procedure yields parameters to minimize the spectral leakage.

1) Adjust $f_{\text{gen}} = m(2f_{\text{g}})$, where m is an integer.
   a) Converter switching frequency f_{sw} restricts the possible choices as $f_{\text{gen}} = f_{\text{sw}}/e$, where e is an integer.
2) Choose $P = f_{\text{gen}}/f_{\text{g}}$ or multiple of it.
   a) $T_{\text{meas}} = P(N/f_{\text{gen}}) = a(1/f_{\text{g}})$, where a is an integer.
   b) This results in $a = N$, and thus, T_{meas} includes exactly $R = N$ fundamental grid cycles and $r = 0$.
3) N can be chosen without restrictions to satisfy the desired measurement characteristics.

As a result of the proposed design procedure, an integer amount of the grid fundamental cycles (and, consequently, its harmonics) is measured. Therefore, the spectral leakage caused by grid voltage harmonics is avoided.

C. Measurement Accuracy

The measurement accuracy can be assessed by its variance σ^2. Higher values indicate increased variability between consecutive measurements and errors around the reference, thus making the measurement system unreliable. In this letter, a smooth impedance Z_{Fit} is used as a reference, produced by a MATLAB's curve-fitting tool from a measurement under ideal grid voltages. The variance can be computed as

$$\sigma^2 = \sum_{f=1}^{\infty}\left[Z_{\text{Fit}}(f) - Z_{\text{meas}}(f)\right]^2 \tag{3}$$

where the variance of the reference is considered as zero. It may be assumed that each dq-domain channel (including cross-couplings) has approximately equal SNR during measurements, and they can be taken equally into account when comparing the measurement results to each other. Thus, the total variance of measurement is computed over the entire dq-domain impedance matrix as

$$\sigma^2_{\text{DQ}} = \sigma^2_{\text{dd}} + \sigma^2_{\text{dq}} + \sigma^2_{\text{qd}} + \sigma^2_{\text{qq}}. \tag{4}$$

IV. Experiments

The experiments are performed using a high-power PHIL setup in accordance with Fig. 1. The system is implemented by two 200-kVA Egston voltage amplifiers and the grid impedance by three-phase inductors. The amplifiers are used to emulate a three-phase grid and a grid-connected converter. The measurement system is described in detail in [8]. In the following experiments, the grid impedance is measured in the dq domain.

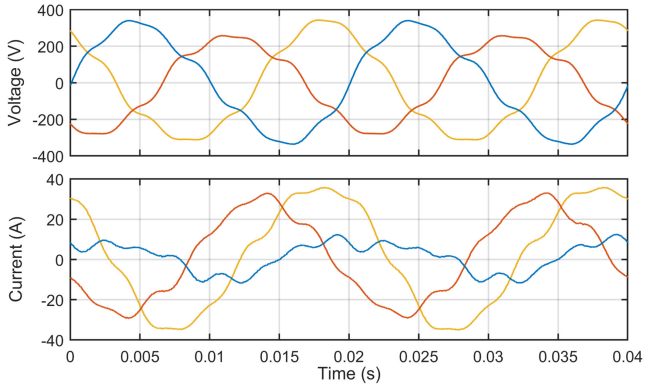

Fig. 3. Polluted grid waveforms without injection.

TABLE I
Nearest Discrete Spectrum Frequency Points to the Grid Harmonics

f (Hz)	50	100	150	300
Below	48.85	97.70	149.00	298.00
Above	51.29	100.15	151.44	300.44

The currents and voltages are measured from the output terminal of the inverter emulator and the data is captured by a measurement card (NI USB-6363). The data are operated by the MATLAB/Data Acquisition Toolbox.

Fig. 3 shows samples of the highly distorted grid voltages (230 V, 50 Hz), under which the experiments are performed. One of the phases is in 20% unbalance and all phases include 5% of the positive-sequence second and seventh harmonics, as well as negative-sequence second and fifth harmonics.

A. Grid Impedance Measurements

Two orthogonal sequences were designed and injected into the references of the current controller. The first sequence had 2047 bits and the second had 4094 bits. Both sequences were generated at 5 kHz, providing 2.44 Hz (5000/2047 Hz) frequency resolution. The number of averaged periods varied between the measurements in order to achieve desired measurement time that minimizes ΔT. The unbalance occurs at 50 and 100 Hz in the dq domain, and the present harmonics at 50, 150, and 300 Hz. As the frequency resolution of the measurements does not produce the discrete spectral line at 50 Hz, the PFE occurs and the harmonics leak to the nearest discrete spectrum frequencies, given in Table I.

Fig. 4 shows the measured grid impedance with two different number of averaged periods. The blue line represents one of the proposed measurement designs ($P = 100$), where the measured data includes an integer amount of the fundamental grid cycles ($R = 2047$, $r = 0$, $\Delta T = 0$). Therefore, the grid impedance measurement does not show any spectral leakage, only the PFE distort the measurement near the grid harmonics, which can be predicted. Red line ($P = 108$) represents design without considering the spectral leakage minimization as the fractional part of grid fundamental cycle occurs in the measured data ($R = 2210$, $r = 0.76$, $\Delta T = 4.8$ ms). Fig. 5 illustrates the time difference between the measurement time for different number of averaged periods and the nearest full period of fundamental

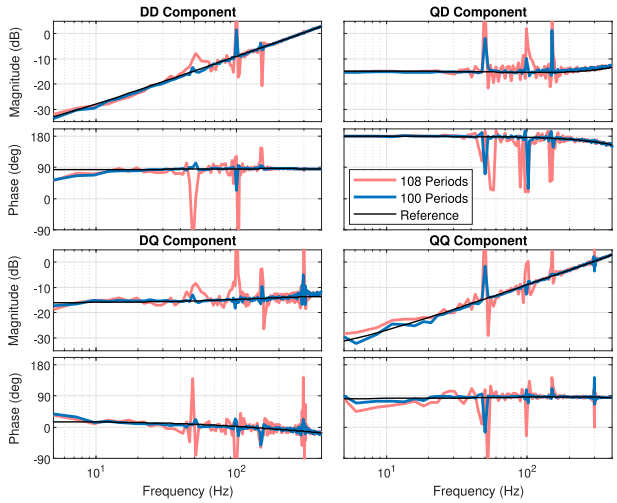

Fig. 4. MIMO measurements of the grid impedance with different averaging.

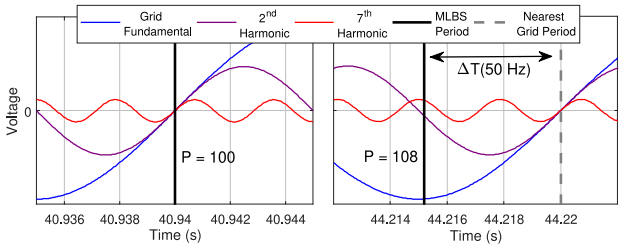

Fig. 5. Time difference between applied MLBS periods $P = 100$ (left), $P = 108$ (right), and grid voltage components.

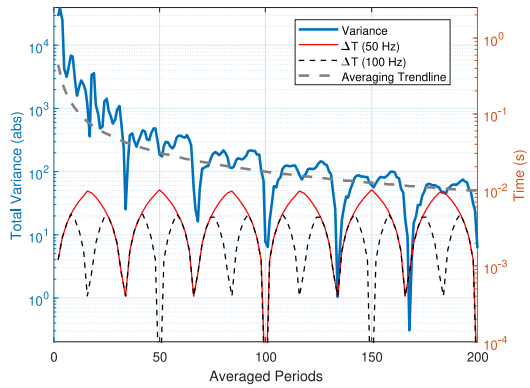

Fig. 6. Variance over different averaging periods.

grid voltage. When $P = 100$ (left), the time difference equals to zero and no spectral leakage occurs. The time difference with $P = 108$ (right) produces spectral leakage, which deteriorates the measurements, as shown in Fig. 4.

Fig. 6 shows the variance, averaging trend line, and the time difference to the grid fundamental cycle $\Delta T(50\,\text{Hz})$ and its second harmonic $\Delta T(100\,\text{Hz})$ with varying number of averaged periods. The local minimums of $\Delta T(50\ \text{Hz})$ give the proposed parameterization to minimize the spectral leakage. The variance follows the averaging trend line otherwise, but the variance is significantly decreased at the local minimums of $\Delta T(50\ \text{Hz})$.

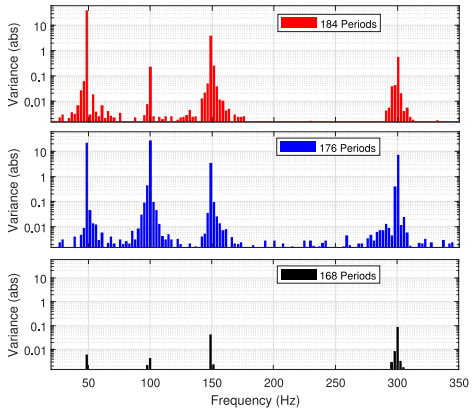

Fig. 7. Variance over frequency spectrum for different numbers of averaged periods.

To illustrate the appearance of the spectral leakage, Fig. 7 shows the measurement variance as a function of the frequency with three different P values, given as

1) $P = 184$ (red bars), chosen from local minimum of $\Delta T(100\ \text{Hz})$, which mitigates the spectral leakage of even-order grid harmonics (here 100 and 300 Hz).
2) $P = 176$ (blue bars) representing design not considering the spectral leakage.
3) $P = 168$ (black bars), chosen from local minimum of both $\Delta T(50\ \text{Hz})$ and $\Delta T(100\ \text{Hz})$, which mitigates the spectral leakage from all grid harmonic frequencies.

V. Conclusion

Wideband identification methods have become popular in the analysis of grid-connected systems. However, recent studies have not considered the undesired spectral leakage that deteriorates the measurements under unbalanced grid conditions or under high harmonic content in the grid voltages. The unbalance and harmonics occurred as periodic oscillations in the measured data and leaked over a wide frequency band during the signal postprocessing. This letter presented methods to mitigate the spectral leakage by adjusting the measurement parameters such that an integer amount of grid-fundamental cycles was included in the measured data. Consequently, the spectral leakage caused by signal processing was avoided, and the frequency responses were obtained with significantly more accuracy. The proposed method was well applicable both in *dq*- and sequence-domain measurements. Experimental measurements based on a high-power PHIL system were shown to demonstrate the effectiveness of the proposed method.

Acknowledgment

This research and testing has been performed using the ERIGrid Research Infrastructure.

References

[1] A. Rygg and M. Molinas, "Apparent impedance analysis: A small-signal method for stability analysis of power electronic-based systems," *IEEE J. Emerg. Sel. Topics Power Electron.*, vol. 5, no. 4, pp. 1474–1486, Dec. 2017.

[2] T. Messo, R. Luhtala, A. Aapro, and T. Roinila, "Accurate impedance model of grid-connected inverter for small-signal stability asssessment in high-impedance grids," *IEEJ J. Ind. Appl.*, vol. 8, pp. 488–492, 2019.

[3] L. Jessen and F. W. Fuchs, "Modeling of inverter output impedance for stability analysis in combination with measured grid impedances," in *Proc. IEEE 6th Int. Symp. Power Electron. Distrib. Gener. Syst.*, 2015, pp. 1–7.

[4] M. Cespedes and J. Sun, "Online grid impedance identification for adaptive control of grid-connected inverters," in *Proc. IEEE Energy Convers. Congr. Expo.*, 2012, pp. 914–921.

[5] J. Schoukens, K. Godfrey, and M. Schoukens, "Nonparametric data-driven modeling of linear systems: Estimating the frequency response and impulse response function," *IEEE Control Syst. Mag.*, vol. 38, no. 4, pp. 49–88, Aug. 2018.

[6] T. Roinila, T. Messo, and E. Santi, "MIMO-identification techniques for rapid impedance-based stability assessment of three-phase systems in dq domain," *IEEE Trans. Power Electron.*, vol. 33, no. 5, pp. 4015–4022, May 2018.

[7] R. Luhtala, T. Roinila, and T. Messo, "Implementation of real-time impedance-based stability assessment of grid-connected systems using MIMO-identification techniques," *IEEE Trans. Ind. Appl.*, vol. 54, no. 5, pp. 5054–5063, Sep./Oct. 2018.

[8] T. Roinila *et al.*, "Hardware-in-the-loop methods for real-time frequency-response measurements of on-board power distribution systems," *IEEE Trans. Ind. Electron.*, vol. 66, no. 7, pp. 5769–5777, Jul. 2019.

[9] C. Li, "Unstable operation of photovoltaic inverter from field experiences," *IEEE Trans. Power Del.*, vol. 33, no. 2, pp. 1013–1015, Apr. 2018.

[10] K. R. Godfrey, *Perturbation Signals for System Identification*. Hemel Hempstead, U.K.: Prentice-Hall, 1993.

[11] G. W. Chang, C. I. Chen, Y. J. Liu, and M. C. Wu, "Measuring power system harmonics and interharmonics by an improved fast Fourier transform-based algorithm," *IET Gener., Transmiss. Distrib.*, vol. 2, no. 2, pp. 193–201, Mar. 2008.

[12] H. Wen, Z. Teng, Y. Wang, B. Zeng, and X. Hu, "Simple interpolated FFT algorithm based on minimize sidelobe windows for power-harmonic analysis," *IEEE Trans. Power Electron.*, vol. 26, no. 9, pp. 2570–2579, Sep. 2011.